Analogue modelling an array of the FitzHugh–Nagumo oscillators

Elena Tamaševičiūtė[a], **Gytis Mykolaitis**[a,b], **Arūnas Tamaševičius**[a]

[a]Nonlinear Electronics Laboratory, Center for Physical Sciences and Technology
A. Goštauto str. 11, Vilnius LT-01108, Lithuania
tamasev@pfi.lt

[b]Department of Physics, Vilnius Gediminas Technical University
Saulėtekio ave. 11, Vilnius LT-10223, Lithuania
gytis@pfi.lt

Received: 28 August 2011 / **Revised:** 24 January 2012 / **Published online:** 24 February 2012

Abstract. The purpose of the paper is to show that analogue electronic modelling is an extremely fast technique compared to conventional digital computing, especially when solving large sets of coupled nonlinear differential equations. An array of thirty FitzHugh–Nagumo type electronic oscillators, modelling dynamics of the brain neurons, is considered. The decrease of time consumption by a factor of several thousands is demonstrated. The work delivers a perspective of how to implement convenient analogue models of complex dynamical networks.

Keywords: analogue modelling, ordinary differential equations, FitzHugh–Nagumo model.

1 Introduction

There are many examples in science and engineering where analogue electrical circuits have been used to model temporal evolution of dynamical systems. This modelling method has been applied to diverse disciplines and areas. The Mackey–Glass delay differential equation, which is well known to describe heamatological disorders, has a simple electronic analogue [1]. A simple electrical circuit has been suggested to imitate the chaotic behaviour of a periodically forced mechanical system [2], described by the Duffing–Holmes ordinary differential equations. Several electrical circuits have been proposed to model the dynamics of neurons [3, 4]. A very interesting solution has been suggested to model mammalian cochlea using high order electrical circuit [5]. One more example is the electrical circuit modelling movement of a spacecraft at the Lagrange point of the astrodynamical Sun–Earth system [6]. It should be emphasized that design of such electrical circuits is not for its own purpose. The analogue circuits mentioned above have been employed for testing various methods developed to control dynamics of the systems, specifically to stabilize steady states [6–9] and periodic orbits [10]. In addition, experiments with electronic analogues can help to better understand the mechanisms

behind the behaviours of complex systems, e.g. the pitch in human perception of the sound [11]. Moreover, the electronic cochlea provides an efficient design of an artificial hearing sensor [12].

One can argue that there is no difference between an analogue electrical circuit, imitating a dynamical system, and an analogue computer, solving corresponding differential equations. We note that any analogue computer is a standard collection of the following main blocks: inverting RC integrators, inverting adders, invertors, inverting and noninverting amplifiers, multipliers, and piecewise linear nonlinear units. Programming of the differential equations on an analogue computer is simply wiring these units according to strictly predetermined rules. Differences between the "intrinsically" analogue electrical circuits, simulating behaviour of dynamical systems, and the conventional analogue computers were discussed by Matsumoto, Chua and Komuro 25 years ago. In this regard, it makes sense to present here an excerpt from their paper [13]: "... the circuit ... is not an analogue computer in the sense that its building blocks are not integrators. They are ordinary circuit elements; namely, resistors, inductors and capacitors. Both current and voltage of each circuit element play a crucial role in the dynamics of the circuit. On the contrary, the variables in a typical analogue computer are merely node voltages of the capacitor-integrator building-block modules, where the circuit current is completely irrelevant in the circuit's dynamic operation. Hence it would be misleading to confuse our circuit as an analogue computer...".

In the present paper, we describe an analogue electronic model, specifically a network of electrical circuits, which imitates dynamics of neurons.

2 Matematical model

The mathematical model is described by a set of $2N$ linearly coupled ordinary nonlinear differential equations [14]:

$$\begin{aligned} \frac{\mathrm{d}x_i}{\mathrm{d}t} &= ax_i - F(x_i) - y_i - c_i + k(x_m - x_i), \\ \frac{\mathrm{d}y_i}{\mathrm{d}t} &= x_i - by_i, \quad i = 1, 2, \ldots, N. \end{aligned} \tag{1}$$

Here the nonlinear function $F(x_i)$ is given by a piece-wise linear approximation:

$$F(x_i) = \begin{cases} d(x_i + 1), & x_i < -1, \\ 0, & -1 \le x \le 1, \\ g(x_i - 1), & x > 1. \end{cases} \tag{2}$$

In Eq. (1) x_m is the mean value of the variables x_i:

$$x_m = \frac{1}{N} \sum_{i=1}^{N} x_i, \tag{3}$$

constant bias c_i is different for every individual oscillator, k is the coupling factor, N is the number of cells, factors a, b, d, and g are defined in [4, 9, 14].

3 Numerical simulation results

Numerical simulations for $N = 30$, $a = 3.4$, $b = 0.15$, $c_i = 3 - 0.05(i-1)$, $d = 60$, $g = 3.4$ were performed using the FreePascal software with the accuracy of 10^{-4}. Typical results are presented in Figs. 1, 2.

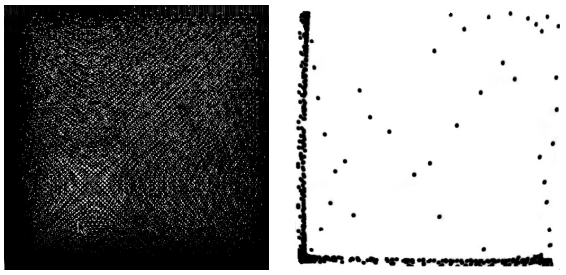

Fig. 1. Non-synchronized case, k=0. Phase portrait ($x_i(t)$ *versus* $x_j(t)$, $i \neq j$) (left). Poincaré section ($x_i(t)$ *versus* $x_j(t)$ at $x_l(t) = 1$, $\mathrm{d}x_l(t)/\mathrm{d}t < 0$, $i \neq j \neq l$) (right).

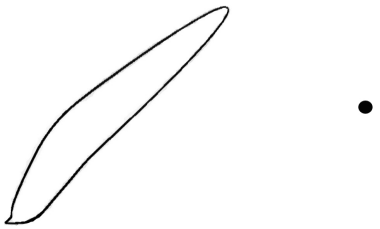

Fig. 2. Synchronized case, $k = 0.7$. Phase portrait ($x_i(t)$ *versus* $x_j(t)$, $i \neq j$) (ellipse). Poincaré section ($x_i(t)$ *versus* $x_j(t)$ at $x_l(t) = 1$, $\mathrm{d}x_l(t)/\mathrm{d}t < 0$, $i \neq j \neq l$) (dot).

4 Electrical circuits

A network of N_i ($i = 1, 2, \ldots, N$) mean-field coupled (star configuration) electronic neurons is sketched in Fig. 3.

Figure 3 (right) depicts the FitzHugh–Nagumo type electronic circuit representing the individual neurons. The neuron cells in the array are slightly mismatched, either by setting different parameters of the LC tanks or by different external dc biasing of the circuit (corresponds constant term c_i in the differential equations), meeting the fact that in real world there are no strictly identical units.

General view of the hardware circuit is shown in Fig. 4. The construction contains four floors. The electronic neurons are on the three floors (10 neurons on each floor), while the all coupling resistors R^* are placed on one floor. Typical output waveform from a single neuron is presented in Fig. 5. Table 1 lists the individual frequencies of all neurons.

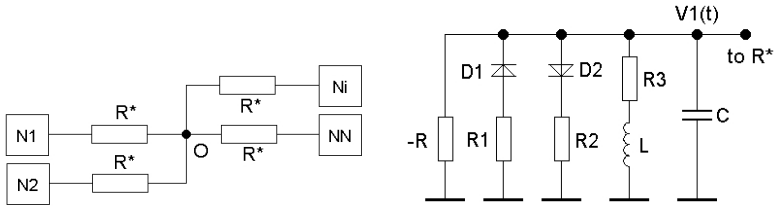

Fig. 3. Block diagram (left) of neurons coupled via resistors R^* to the coupling node O. Circuit diagram (right) of a single electronic neuron. Element labelled with $-\mathrm{R}$ is a negative resistance, implemented by means of negative impedance converter [15].

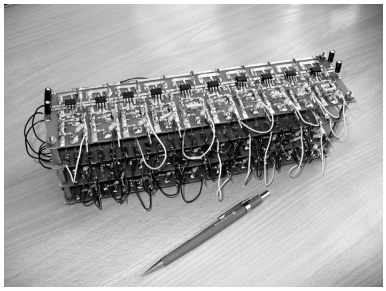

Fig. 4. Hardware prototype of the array of 30 electronic neurons. Dimensions $\mathrm{W} \times \mathrm{H} \times \mathrm{D} = 270$ mm $\times$ 85 mm $\times$ 65 mm.

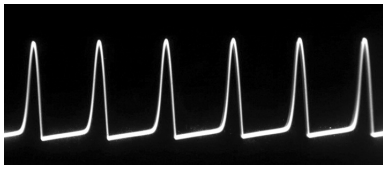

Fig. 5. Output waveform from a single electronic neuron $V_1(t)$. Spike amplitude $\approx$ 10 V, interspike interval $\approx$ 75 μs (frequency $\approx$ 13 kHz).

Table 1. Frequencies of the individual electronic neurons.

No.	f, kHz	No.	f, kHz	No.	f, kHz	No.	f, kHz	No.	f, kHz
1	12.280	7	12.659	13	12.872	19	13.393	25	13.668
2	12.299	8	12.717	14	12.982	20	13.394	26	13.702
3	12.340	9	12.769	15	13.077	21	13.472	27	13.727
4	12.412	10	12.776	16	13.128	22	13.487	28	13.773
5	12.482	11	12.830	17	13.237	23	13.570	29	13.801
6	12.543	12	12.856	18	13.283	24	13.626	30	13.802

5 Analogue simulation results

In the case of weak coupling (large R^*), the neurons are spiking independently at their individual frequencies (see Table 1). The intricate phase portrait and multi-dot Poincaré section (Fig. 6) do confirm this statement. In all analogue simulations the exposure time was fixed at $1/8$ s $= 0.125$ s. This yielded 1500 snapped periods of the waveforms in the phase portraits and 1500 snapped dots in the Poincaré sections.

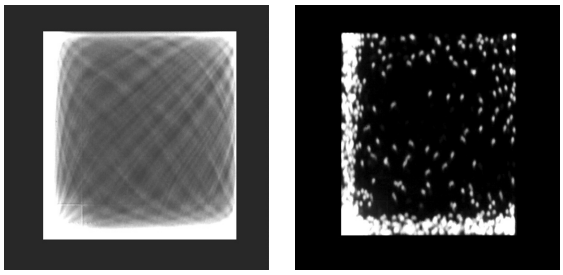

Fig. 6. Non-synchronized case. Phase portrait ($V_i(t)$ *versus* $V_j(t)$, $i \neq j$) (left). Poincaré section ($V_i(t)$ *versus* $V_j(t)$ at $V_l(t) = 1$ V, $\mathrm{d}V_l(t)/\mathrm{d}t < 0$, $i \neq j \neq l$) (right).

For stronger coupling (smaller R^*) all neurons become fully synchronized, i.e. phase-locked, as is evident from the phase portrait, displaying a simple ellipse and a single dot in the Poincaré section (Fig. 7).

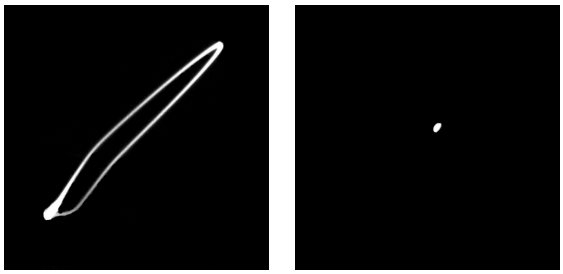

Fig. 7. Synchronized case. Phase portrait ($V_i(t)$ *versus* $V_j(t)$, $i \neq j$) (ellipse). Poincaré section ($V_i(t)$ *versus* $V_j(t)$ at $V_l(t) = 1$ V, $\mathrm{d}V_l(t)/\mathrm{d}t < 0$, $i \neq j \neq l$) (dot).

We note that in order to display analogue simulation results, presented in Figs. 6, 7 from the hardware circuit in Fig. 4, one needs some special electronic equipment. Namely, an oscilloscope with an X input (horizontal channel) and an Y input (vertical channel) is required to take the phase portraits. An X/Y channelled oscilloscope with an additional feature of external beam modulation (Z input) is necessary (along with an external pulse generator) to plot the Poincaré sections. However, this equipment may not be available in a standard laboratory.

To get around the problems, a standard multi-channel (at least 2-channel) oscilloscope can be used for displaying the waveforms $V_i(t)$ and $V_j(t)$ from the pairs of neurons, $i \neq j$, as shown in Fig. 8 and Fig. 9. The internal horizontal sweep saw-tooth generator of the oscilloscope should be synchronized with one of the input waveform, either with $V_i(t)$ or with $V_j(t)$. The waveforms can be inspected visually on the screen of the oscilloscope and snapshots can be taken photographically or by means of a camera, if necessary.

However, this method (also the previously described phase portraits and the Poincaré sections techniques) requires checking the state of all different pairs of the oscillators,

$i \neq j$. It may be time consuming procedure, since there is a lot of different pairs in the network of N neurons, given by the number of combinations:

$$C_N^2 = \frac{N!}{2!(N-2)!} = \frac{N(N-1)}{2}. \tag{4}$$

In the case of $N = 30$ there are 435 pairs.

Therefore we propose one more very simple alternative technique for checking the network, whether it is in either non-synchronized or synchronized state. One needs a simple single-channel oscilloscope only. Instead of checking all the 435 pairs, the method makes use of a single measurement only. Examples are shown in Fig. 10 and Fig. 11. In the non-synchronized case the mean-field voltage $V_m(t)$ taken from the node O (Fig. 3 left) has relatively low amplitude (< 1 V). Moreover, the oscilloscope cannot be synchronized with it (Fig. 10). In contrast, the synchronized $V_m(t)$ has relatively high amplitude (> 10 V), exhibits simple spiking periodic waveform, similar to that of a single neuron (Fig. 5). Therefore $V_m(t)$ is easily synchronized on the screen of the oscilloscope (Fig. 11).

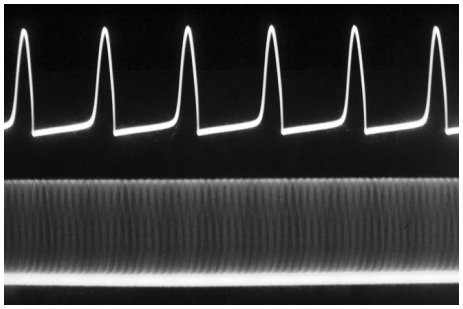

Fig. 8. Waveforms $V_i(t)$ (top) and $V_j(t)$ (bottom), $i \neq j$, non-synchronized case. Oscilloscope is synchronized internally with $V_i(t)$.

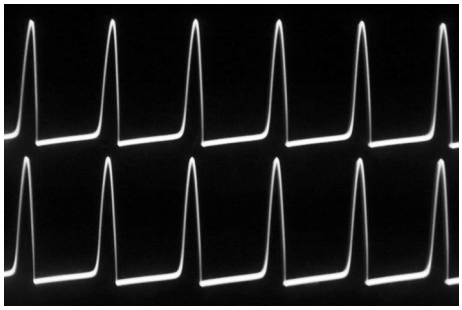

Fig. 9. Waveforms $V_i(t)$ (top) and $V_j(t)$ (bottom), $i \neq j$, synchronized case. Oscilloscope is synchronized internally with $V_i(t)$.

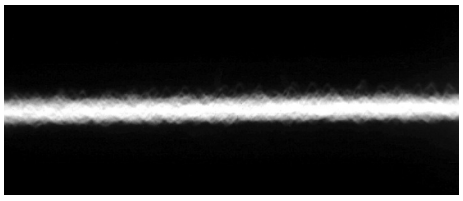

Fig. 10. Waveform of the mean voltage $V_m(t)$, non-synchronized case. Oscilloscope is unable to synchronize with the non-periodic waveform.

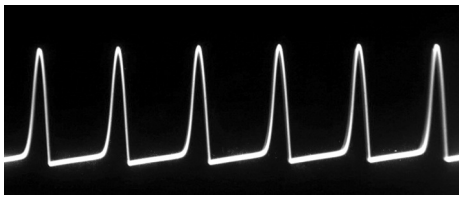

Fig. 11. Waveform of the mean voltage $V_m(t)$, synchronized case. Oscilloscope easily synchronizes with this simple periodic waveform.

6 Comparing numerical and analogue simulations

One of the most important characteristics of any modelling technique is the simulation time required to obtain the result. This parameter is given in Table 2 to compare the two considered methods, numerical versus analogue. Waveforms and phase portraits contain 1500 periods of dimensionless variable $x_1(t)$ and voltage $V_1(t)$, in the numerical simulations and analogue modelling, respectively. The Poincaré sections are plotted using 1500 dots.

Table 2. Time elapsed getting the result.

Plot type	Numerical[1]	Numerical[2]	Analogue
Waveform $V(t)$	8 min. 10 s	9 min. 00 s	0.125 s
Phase portait	8 min. 10 s	9 min. 00 s	0.125 s
Poincaré section	8 min. 55 s	8 min. 55 s	0.125 s

[1]PC with 1.7 GHz CPU, FreePascal, Euler integration method, accuracy 10^{-4}; screen display.
[2]The same PC, software and integration method; screen display + writing to data file.

7 Concluding remarks

We have designed, built and investigated an electrical network consisting of 30 FitzHugh–Nagumo oscillators and have demonstrated the synchronization effect. The following estimates were taken into account when choosing the number of oscillators. The minimal number of units in a star configuration is 3 [14]. Our network consists of 30 neurons, thus can be treated as a large array. On the other hand, 30 oscillators is rather small amount of units that can be easily built for a scientific laboratory.

It is evident from Table 2 that the analogue simulation technique has a big advantage against the numerical simulation from the point of view of time consumption. This is due to fact that analogue simulation uses parallel processing; it is independent on N, the number of the units. Meanwhile, numerical simulation employs series processing; the processing time is proportional to N. Moreover, analogue simulations operate with continuous flows on a continuous time scale, in contrast to numerical methods, which require discrete time and other variables. Analogue modelling, described in the paper, is based on some specific analogue electrical circuit for a given dynamical system or given differential equation. Despite its limitation to specific systems or equations, electrical circuits have an attractive advantage of simplicity and cheapness. Such circuits comprise rather small number of simple electrical components: resistors, capacitors, inductors, semiconductor diodes, may include operational amplifiers. The analogue modelling method using simple electrical circuits can be applied to many other dynamical systems, especially to complex networks.

Ackowledgments

The authors are grateful to Ruedi Stoop from the Institute of Neuroinformatics of the University of Zürich and the ETH Zürich for useful advices.

References

1. A. Namajūnas, K. Pyragas, A. Tamaševičius, An electronic analog of the Mackey–Glass system, *Phys. Lett. A*, **201**(1), pp. 42–46, 1995.
2. E. Tamaševičiūtė, A. Tamaševičius, G. Mykolaitis, S. Bumelienė, E. Lindberg, Analogue electrical circuit for simulation of the Duffing–Holmes equation, *Nonlinear Anal. Model. Control*, **13**(2), pp. 241–252, 2008.
3. S. Binczak, V.B. Kazantsev, V.I. Nekorkin, J.M. Bilbaut, Experimental study of bifurcations in modified FitzHugh–Nagumo cell, *Electron. Lett.*, **39**(13), pp. 961–962, 2003.
4. E. Tamaševičiūtė, A. Tamaševičius, G. Mykolaitis, S. Bumelienė, R. Kirvaitis, R. Stoop, Electronic analog of the FitzHugh–Nagumo neuron model and noninvasive control of its steady state, in: *Proc. of the 17th Int. Workshop on Nonlinear Dynamics of Electronic Systems, 21–24 June, 2009, Rapperswil, Switzerland*, pp. 138–141.
5. S. Martignoli, J.J. van der Vyver, A. Kern, Y. Uwate, R. Stoop, Analog electronic cochlea with mammalian hearing characteristics, *Appl. Phys. Lett.*, **91**(6), 064108, 2007.
6. A. Tamaševičius, E. Tamaševičiūtė, G. Mykolaitis, S. Bumelienė, R. Kirvaitis, Stabilization of saddle steady states of conservative and weakly damped dissipative dynamical systems, *Phys. Rev. E*, **82**(2), 026205, 2010.
7. A. Namajūnas, K. Pyragas, A. Tamaševičius, Analog techniques for modeling and controlling the Mackey–Glass system, *Int. J. Bifurcation and Chaos*, **7**(4), pp. 957–962, 1997.
8. A. Tamaševičius, E. Tamaševičiūtė, G. Mykolaitis, S. Bumelienė, Switching from stable to unknown unstable steady states of dynamical systems, *Phys. Rev. E*, **78**(2), 026205, 2008.
9. A. Tamaševičius, E. Tamaševičiūtė, G. Mykolaitis, S. Bumelienė, R. Kirvaitis, R. Stoop, Neural spike suppression by adaptive control of an unknown steady state, in: C. Alippi et al. (Eds.), *Artificial Neural Networks – ICANN 2009*, Part I, Lect. Notes Comput. Sci., Vol. 5768, 2009, pp. 618–627.
10. A. Tamaševičius, G. Mykolaitis, V. Pyragas, K. Pyragas, Delayed feedback control of periodic orbits without torsion in nonautonomous chaotic systems: Theory and experiment, *Phys. Rev. E*, **76**(2), 026203, 2007.
11. S. Martignoli, R. Stoop, Local cochlear correlations of perceived pitch, *Phys. Rev. Lett.*, **105**(4), 048101, 2010.
12. R. Stoop, T. Jasa, Y. Uwate, S. Martignoli, From hearing to listening: design and properties of an actively tunable electronic hearing sensor, *Sensors*, **7**(12), pp. 3287–3298, 2007.
13. T. Matsumoto, L.O. Chua, M. Komuro, The double scroll, *IEEE Trans. Circuits Syst.*, **32**(8), pp. 797–818, 1985.
14. A. Tamaševičius, S. Bumelienė, E. Tamaševičiūtė, G. Mykolaitis, R. Kirvaitis, Desynchronization of mean-field coupled oscillators by remote virtual grounding, in: *Proc. of the 18th Int. Workshop on Nonlinear Dynamics of Electronic Systems, 26–28 May, 2010, Dresden, Germany*, pp. 30–33.
15. P. Horowitz, W. Hill, *The Art of Electronics*, Cambridge University Press, Cambridge, 1993.